Relationship of oceanic whitecap coverage to wind speed and wind history

Adrian Callaghan,[1] Gerrit de Leeuw,[2,3,4] Leo Cohen,[5] and Colin D. O'Dowd[6]

[1]   Sea surface images obtained during the 2006 Marine Aerosol Production (MAP) campaign in the North East Atlantic were analysed for values of percentage whitecap coverage (W). Values of W are presented for wind speeds up to *circa* 23 m s^{-1}. The W data were divided into two overlapping groups and a piecewise, wind-speed-only parameterization of W is proposed that is valid for wind speeds between 3.70 m s^{-1} and 23.09 m s^{-1}. Segregation of data points based upon a 2.5 hour wind history acted to decrease data scatter at wind speeds above approximately 9.25 m s^{-1}. At these wind speeds W values were greater for decreasing wind speeds than for increasing wind speeds. No clear wind history effect was observed at wind speeds below 9.25 m s^{-1}. **Citation:** Callaghan, A., G. de Leeuw, L. Cohen, and C. D. O'Dowd (2008), Relationship of oceanic whitecap coverage to wind speed and wind history, *Geophys. Res. Lett.*, *35*, L23609, doi:10.1029/2008GL036165.

1.   Introduction

[2]   Whitecaps are the surface signature of buoyant bubble plumes caused by energetic breaking wind-generated gravity waves and they affect a wide range of oceanographically related processes. The air-sea transfer of gases is enhanced due to turbulence and bubbles created in the wave breaking process and due to the effect of bubbles [*Woolf*, 2005]. The bubble-bursting processes associated with whitecaps, which produce film and jet droplets, are the primary source of the marine aerosol away from the surf zone [*O'Dowd and De Leeuw*, 2007]. The high albedo of whitecaps means that they provide a cooling influence on the earth's climate [*Frouin et al.*, 2001]. Their presence on the sea surface has to be accounted for in the atmospheric correction for the retrieval of ocean colour information from remote sensing satellites [*Gordon*, 1997].

[3]   Wind stress is the dominant force that affects W. Many studies have provided open ocean datasets which have been used to develop parameterizations of W in terms of wind speed alone. We refer the reader to a comprehensive review of the whitecap literature by both *Lewis and Schwartz* [2004] and *Anguelova and Webster* [2006]. In this paper we report on measurements of W made in the North Atlantic as part of the Marine Aerosol Production (MAP) campaign from the summer of 2006. A preliminary report on a subset of the MAP W data is given by *Callaghan et al.* [2007], but the data presented here supersede those data.

2.   Study Area and Methodology

[4]   The MAP field campaign took place on board the Irish R.V. Celtic Explorer from 11 June to 5 July, 2006. Images collected in June on days 17, 19, 20, 21, 22, 27 and 28, were selected to cover the widest range of wind speeds and analysed for W. The ship's location varied inside a geographical area defined by 9.5°W, 13°W, 55.5°N and 57.5°N. Fetch conditions were practically unlimited except on June 28th and the morning of June 20th when minimum fetch conditions were on average 200km and 500km respectively. Following *Carter* [1982], it was estimated that the wave field may have been duration limited.

[5]   Images were taken every 2 seconds in daylight hours using a video system mounted in a fixed position on the ship 19m above sea level. The video was positioned 84° from the nadir and had a focal length of 50mm. The images had an initial pixel resolution of 768 X 576 but were cropped to 715 X 535 due to inconsistent image borders which gave an image footprint of approximately 4997m^2. In total 43158 images were analysed for W which yielded 107 W data points. Images were processed using the Automated Whitecap Extraction (AWE) algorithm described by *Callaghan and White* [2008]. The AWE algorithm examines differences in the intensity values of each image and uses techniques based on derivative analysis to automatically determine the most appropriate threshold intensity with which to identify whitecaps only. Following *Callaghan et al.* [2008] and *Callaghan and White* [2008], on the order of hundreds of images should be analysed to achieve convergent values of W. All suitable images in a half hour period were analysed to produce a single W data point. Images that contained the horizon were manually removed before analysis. Only half hour periods with images that were not contaminated by sun glint or sky reflection were analysed. The minimum, maximum and average number of images analysed for each W data point were 100, 782 and 403 respectively. The number of images suitable for analysis decreased with increasing wind speed.

[6]   Wind speed and direction were measured by the ship's anemometer 27m above the sea surface. Due to technical

---
[1]Department of Earth and Ocean Sciences, National University of Ireland, Galway, Ireland.
[2]Department of Physics, University of Helsinki, Helsinki, Finland.
[3]Climate Change Unit, Finnish Meteorological Institute, Helsinki, Finland.
[4]TNO Built Environment and Geosciences, Utrecht, Netherlands.
[5]TNO Defense and Security, Hague, Netherlands.
[6]School of Physics and Centre for Climate and Air Pollution Studies, Environmental Change Institute, National University of Ireland, Galway, Ireland.
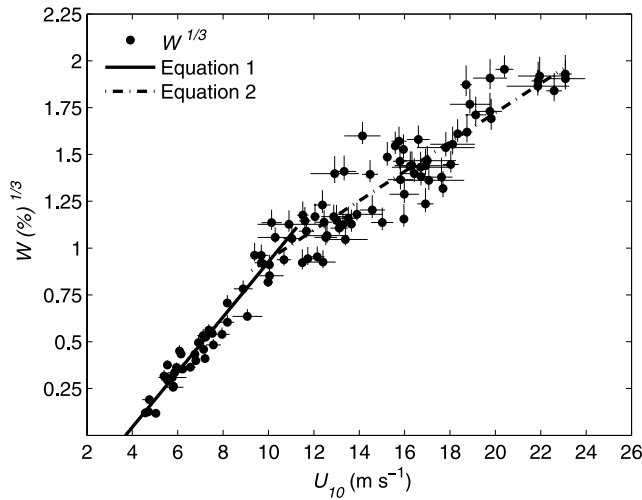
Figure 1. The variation of $W^{1/3}$ with U_{10}. The solid line represents equation (1) and the dot-dash line represents equation (2). The vertical error bars correspond to the measurement error associated with the image processing algorithm. The horizontal error bars correspond to ±1 standard error of U_{10}.

difficulties, coincident water temperature (T_w) and air temperature (T_a) measurements were only made for 44 whitecap-wind speed data point pairs. Measured T_w and T_a values ranged between $12.99°C–13.77°C$ and $9.29°C–13.43°C$ respectively. The atmospheric stability ($\Delta T = T_w - T_a$) was always positive and ranged between $0.13°C–3.86°C$ indicating unstable atmospheric conditions. Since T_w and T_a were not available for all wind speed measurements U_{10} was calculated using the wind profile power law, where $U_{10} = U_{27}\,(10/27)^{1/7}$ [*Blackadar*, 1997], and averaged to provide half hourly values. For the available 44 temperature measurements the neutral wind speed, U_{10N}, was calculated following *Hsu* [2003]. U_{10N} values were found to be larger than U_{10} by between 5.95% and 11.21% and the differences decreased with increasing wind speed. U_{10} values were not corrected for the effects of flow distortion introduced by the research vessel.

3. Results and Discussion

3.1. Data Presentation and Parameterization

[7] Following *Monahan and Lu* [1990], W can be related to U_{10} with a power law of form $W = c_1(U_{10} + c_0)^3$. This was achieved by plotting $W^{1/3}$ against U_{10} and performing a linear regression resulting in $W^{1/3} = m_1 U_{10} + m_0$ which was then rearranged and cubed. When c_0 is negative it represents the minimum wind speed necessary for the onset of detectable whitecapping.

[8] Figure 1 shows a plot of $W^{1/3}$ against U_{10}. The data were initially fitted with a single regression but an examination of the fit residuals revealed a poor goodness of fit. Therefore, the data were divided into two overlapping groups and a regression was performed on each group. The first group consisted of all W data points measured at wind speeds below 11.25 m s^{-1}. The second group consisted of all W data points measured at wind speeds above

9.25 m s^{-1}. The resultant cubed relationships, valid wind speed ranges and r^2 values are given as:

$$W = 3.18 \times 10^{-3}(U_{10} - 3.70)^3; \quad 3.70 < U_{10} \leq 11.25; \quad r^2 = 0.940 \tag{1}$$

$$W = 4.82 \times 10^{-4}(U_{10} + 1.98)^3; \quad 9.25 < U_{10} \leq 23.09; \quad r^2 = 0.842 \tag{2}$$

The vertical error bars in Figure 1 represent the measurement error associated with the AWE image processing algorithm and they represent approximately +20% and −10% of each W value. The horizontal error bars represent ±1 standard error of U_{10}. Equations (1) and (2) intersect at a wind speed of 10.18 m s^{-1} and could be combined to form a continuous parameterization of W for wind speeds between 3.70 m s^{-1} to 23.09 m s^{-1}. The point of intersection represents a change in the relationship between W and U_{10} which is similar in value to the wind speed needed for the onset of spume droplet production which lies between 9 m s^{-1} and 11 m s^{-1} [*Monahan et al.*, 1986, 1983]. The production of spume droplets indicates a somewhat altered or additional wind wave interaction mechanism where the wind is strong enough to tear water away from the wave crests which may be responsible for the change in the dependence of W on U_{10} as seen in Figure 1. From equation (1) the minimum wind speed needed for the onset of detectable whitecapping in this study occurred at approximately 3.70 m s^{-1}.

[9] Both the data scatter and the range of the W error bars are seen to increase with increasing wind speed. Increased scatter may be due to increased wind variability, decreased stability of the ship which could have affected wind speed measurements and a reduced number of available images for analysis at higher wind speeds. The magnitude of the U_{10} error bars increases with increasing wind speed reflecting the increased wind variability. The average number of images analysed per W data point at wind speeds below 10ms^{-1} was 579 and 314 for wind speeds greater than 10ms^{-1}.

3.2. Effect of Wind History

[10] Wave age is the ratio of the speed of the waves at the peak of the wind wave frequency spectrum (c_p) and U_{10} and it can be used as an indicator of sea state development. *Sugihara et al.* [2007] found that at a given wind speed W was proportional to wave age in conditions of a pure wind sea. When W was plotted against U_{10}, at a given wind speed the W data points corresponding to "older" seas lay above those measured in younger seas. Somewhat similarly, but based on visual estimates of wave development, *Stramska and Petelski* [2003] observed that W was higher in developed seas than in undeveloped seas.

[11] Wave age and sea state in the open ocean will usually depend upon wind history. Periods of decreasing wind speed should be broadly analogous to more developed seas with a relatively high wave age and periods of increasing wind speed should be broadly analogous to less developed seas with a relatively low wave age. The wind history or wind acceleration was calculated in a manner similar to
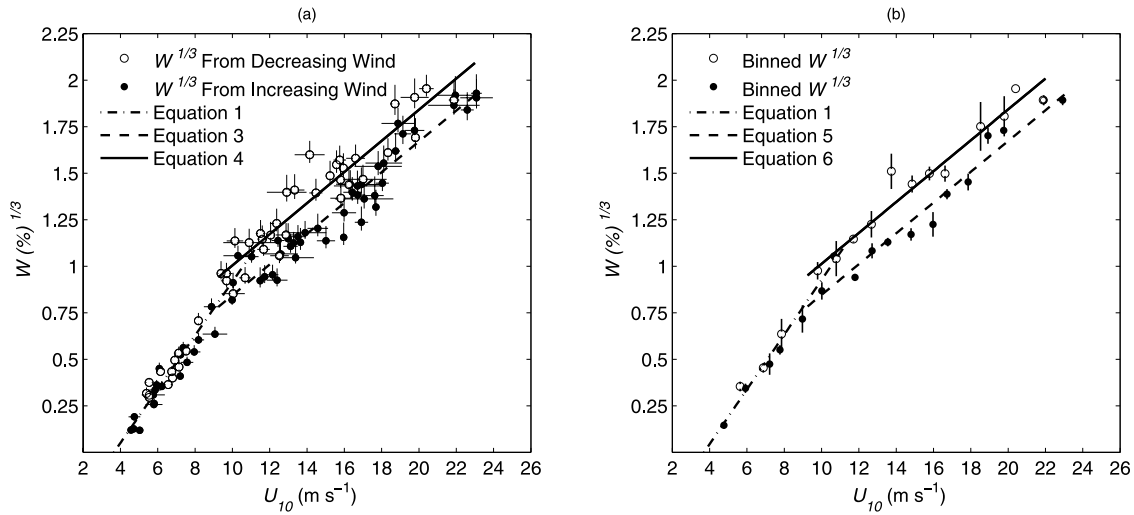
Figure 2. The variation of $W^{1/3}$ with U_{10}. (a) W data points are segregated in terms of a 2.5 hour wind history. Black dots indicate W from periods of increasing wind speed. Open circles indicate W from periods of decreasing wind speed. The dot-dash line, dashed line and solid line represent equations (1), (3), and (4) respectively. The error bars are as in Figure 1. (b) Same as Figure 2a except data have been binned into 1m s^{-1} intervals and show ±1 standard error. Dashed and solid lines represent equations (5) and (6) respectively.

Hanson and Phillips [1999] as $\bar{a} = \Delta\overline{U_{10}}/\Delta t$ where $\overline{U_{10}}$ represents the wind speed averaged over the wind history time period and Δt represents the time interval between each wind speed measurement.

[12] Figure 2a displays the W data segregated into periods of increasing wind speed (positive $\bar{a}$ - black dots) and decreasing wind speed (negative $\bar{a}$ - open circles) over a 2.5 hour wind history period. Figure 2b show these data binned into 1 m s^{-1} intervals. At wind speeds below approximately 9 m s^{-1} no obvious wind history trend is evident whereas at higher wind speeds it appears that two distinct groups of W data emerge. The lack of any wind history effect at lower wind speeds may reflect the decreased variability of the wind at these values. The standard deviation of the wind acceleration was almost three times less for wind speeds lower than 9 m s^{-1} than for wind speeds above 9 m s^{-1}. At wind speeds above approximately 9m s^{-1}, W is generally larger for periods of decreasing wind speed than for periods of increasing wind speed. Given our assumptions in the previous paragraph this is similar to the findings of *Sugihara et al.* [2007] and *Stramska and Petelski* [2003]. It is noted that *Stramska and Petelski* [2003] did include 5 W data points measured during decreasing wind speeds in their undeveloped sea state category. These 5 data points were at wind speeds below 8 m s^{-1} and two of the five were comparable in magnitude to W from developed seas.

[13] The dashed and solid lines in Figure 2a represent the regressions for periods of increasing wind and decreasing wind respectively. The resultant cubed regressions, valid wind speed ranges and r^2 values are given as

$$W = 5.66 \times 10^{-4}(U_{10} + 0.20)^3; \ 9.25 < U_{10} \leq 23.09;$$
$$r^2 = 0.924 \tag{3}$$

$$W = 5.86 \times 10^{-4}(U_{10} + 2.00)^3; \ 9.25 < U_{10} \leq 21.88;$$
$$r^2 = 0.893 \tag{4}$$

The regressions on the binned data were almost identical and they are given as

$$W = 5.65 \times 10^{-4}(U_{10} + 0.23)^3; \ 9.25 < U_{10} \leq 23.09;$$
$$r^2 = 0.958 \tag{5}$$

$$W = 5.71 \times 10^{-4}(U_{10} + 2.21)^3; \ 9.25 < U_{10} \leq 21.88;$$
$$r^2 = 0.956 \tag{6}$$

Given the lack of trend in the segregated W data points in relation to wind history at low wind speeds, equation (1) could be coupled with equations (3) and (4) to provide a wind speed only parameterization of W for wind speeds between 3.70 m s^{-1} and 23.09 m s^{-1} for increasing and decreasing winds respectively in terms of a 2.5 hour wind history. Small changes in valid wind speed range for equation (1) would then be needed to ensure continuity.

[14] To test if the W data points from increasing and decreasing wind histories above 9.25m s^{-1} were significantly different for both unbinned and binned data, an analysis of variance (ANOVA) was carried out using the "anova1.m" function in Matlab. First, the wind speed dependence was removed by calculating the residuals between the W data points and equation (2). The ANOVA was calculated using these fit residuals for both unbinned and binned data and resulted in p values on the order of 1×10^{-10} and 2×10^{-4} respectively. This indicates that the differences between the two datasets are highly significant and demonstrates the important role wind history played in influencing the variation of W. From Figure 2a it can be seen that equations (3) and (4) have almost identical slopes but that the c_0 coefficient is larger by 1.8 m s^{-1} in equation (4) than in equation (3). Similarly *Sugihara et al.* [2007] found that wave age had little effect on the slope of the relationship between W and U_{10} but for W measured in a pure wind sea, older seas introduced a positive offset of 0.7 m s^{-1} in the value of c_0.
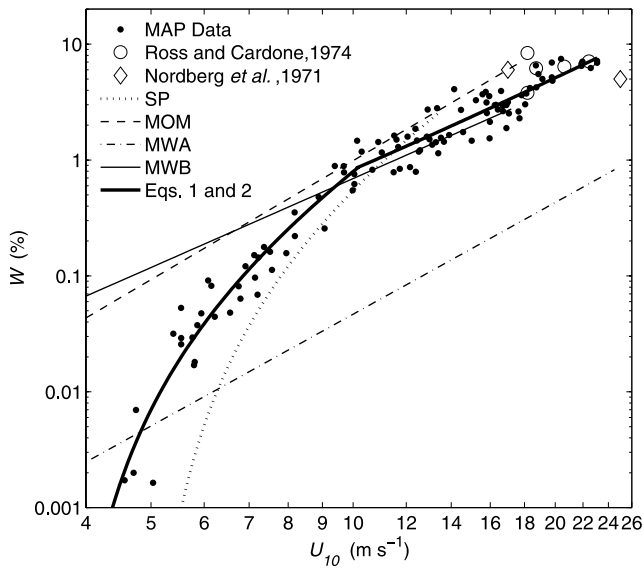
Figure 3. The variation of W with U_{10} and a presentation of previous literature values and parameterizations. Solid dots are MAP W data points. Symbols correspond to data points at wind speeds greater than 17m s^{-1} taken from *Ross and Cardone* [1974] (open circles) and *Nordberg et al.* [1971] (open diamonds). Previous open ocean wind speed whitecap parameterizations plotted over their valid wind speed ranges include *Stramska and Petelski* [2003] (SP, $W = 4.18 \times 10^{-5}(U_{10} - 4.93)^3$), *Monahan and O'Muircheartaigh* [1980] (MOM, $W = 3.84 \times 10^{-4}U_{10}^{3.41}$), *Monahan and Woolf* [1989] (MWA, $W_A = 2.92 \times 10^{-5}U_{10}^{3.204}e^{0.198\Delta T}$ evaluated at $\Delta T = 0$), and *Monahan and Woolf* [1989] (MWB, $W_B = 1.95 \times 10^{-3}U_{10}^{2.55}e^{0.0861\Delta T}$ evaluated at $\Delta T = 0$).

3.3. Comparison With Previous Studies

[15] Figure 3 displays 7 W values measured at wind speeds greater than or equal to 17m s^{-1} from *Nordberg et al.* [1971] and *Ross and Cardone* [1974]. Both these studies divided their W values into two parts consisting of whitecaps and foam streaks. They noted the presence of foam streaks above about 13 m s^{-1} and the ratio of the area of foam streaks to whitecaps increased with increasing wind speed and quickly grew larger than 1. Their W data points included in Figure 3 represent the whitecap only measurement and thus exclude the contribution from foam streaks. Only Stage A and Stage B whitecaps [*Monahan and Lu*, 1990] were measured with the AWE algorithm with no contribution from foam streaks. The MAP values above 17m s^{-1} agree well with the values from other studies.

[16] All previous wind speed only parameterizations of W in Figure 3 have been plotted for the range of wind speeds over which they were determined. These include parameterizations from *Stramska and Petelski* [2003] (hereinafter SP), *Monahan and O'Muircheartaigh* [1980] (hereinafter MOM) and two from *Monahan and Woolf* [1989] (hereinafter MWA and MWB). MOM, SP and MWB represent the variation of the total whitecap coverage (stages A and B) with U_{10} but MWA represents the contribution from stage A whitecaps only. The W MAP data compare favourably to previous open ocean parameterizations of W from stage A and B whitecaps. Figure 3 corroborates our contention that

the video derived MAP W data are measures of the contribution from both stage A and stage B whitecaps.

[17] At lower wind speeds, the trend and magnitude of the MAP data follow SP more closely than the other W parameterizations. This could be due to the image processing techniques used in these studies. SP was determined using digital image analysis while MOM and MWB were determined from film photography using the method outlined by *Monahan* [1969]. Briefly, Monahan's method involved projecting each photograph onto a large piece of card and excising the whitecaps. The ratio of the weight of these whitecap cut-outs to the total weight of the card gave a value of W for each photograph. Digital image processing techniques are able to resolve the patchy appearance of stage B whitecaps whereas the manual method developed by *Monahan* [1969] included the bubble free spaces present in stage B whitecaps in the overall W value [*Stramska and Petelski*, 2003]. At lower wind speeds when the number of breaking wave events is relatively small, the differences in W derived from both methods may be largest.

4. Conclusions

[18] Measurements of W from the North East Atlantic were made in wind speeds that reached ≈ 23 m s^{-1}. $W^{1/3}$ scaled linearly with U_{10} and displayed an apparent change in slope at wind speeds ≈ 10 m s^{-1}. The W data points were divided into two groups and a piecewise wind-speed-only parameterization of W was found. The transition in slope between $W^{1/3}$ and U_{10} coincides with the wind speed needed for spume droplet formation and may reflect an altered mechanism of interaction between wind and waves which is manifested in whitecap production.

[19] A lack of air and water temperature data for all W values did not allow the correction of U_{10} to the preferable quantity, U_{10N}. The available temperature data indicated that U_{10N} may have been between 5.95% and 11.21% higher than U_{10}. Using U_{10N} in place of U_{10} in equations (1) and (2) could have decreased W on average by between 18.82% and 31.16%.

[20] The effect of a 2.5 hour wind history was found to significantly decrease data scatter above *circa* 9.25 m s^{-1}. Above 9.25 m s^{-1} W was generally found to be larger in periods of decreasing wind speeds than in periods of increasing wind speeds. Using wind history as an indication of sea state development, this result suggests that W is larger in developed seas than in developing seas. This indicates the benefit of having an estimation of sea state when parameterizing W in terms of U_{10} alone.

References

Anguelova, M. D., and F. Webster (2006), Whitecap coverage from satellite measurements: A first step toward modeling the variability of oceanic whitecaps, *J. Geophys. Res.*, *111*, C03017, doi:10.1029/2005JC003158.
Blackadar, A. K. (1997), *Turbulence and Diffusion in the Atmosphere: Lectures in Environmental Sciences*, Springer, Berlin.

Callaghan, A. H., and M. White (2008), Automated processing of sea sur-
face images for the determination of whitecap coverage, *J. Atmos. Ocea-
nic Technol.*, doi:10.1175/2008JTECH0634.1, in press.
Callaghan, A. H., G. de Leeuw, and L. H. Cohen (2007), Observations
of oceanic whitecap coverage in the North Atlantic during gale force
winds, in *Nucleation and Atmospheric Aerosols*, edited by C. D.
O'Dowd and P. E. Wagner, pp. 1088–1092, Springer, Dordrecht,
Netherlands.
Callaghan, A. H., G. B. Deane, and M. D. Stokes (2008), Observed phy-
sical and environmental causes of scatter in whitecap coverage values in a
fetch-limited coastal zone, *J. Geophys. Res.*, 113, C05022, doi:10.1029/
2007JC004453.
Carter, D. J. T. (1982), Prediction of wave height and period for a constant
wind velocity for the JONSWAP results, *Ocean. Eng.*, 9, 17–33.
Frouin, R., S. F. Iacobellis, and P.-Y. Deschamps (2001), Influence of
oceanic whitecaps on the global radiation budget, *Geophys. Res. Lett.*,
28, 1523–1526.
Gordon, H. R. (1997), Atmospheric correction of ocean color imagery in
the Earth Observing System era, *J. Geophys. Res.*, 102, 17,081–17,106.
Hanson, J. L., and O. M. Phillips (1999), Wind sea growth and dissipation
in the open ocean, *J. Phys. Oceanogr.*, 29, 1633–1648.
Hsu, S. A. (2003), Estimating overwater friction velocity and exponent
of power law wind profile from gust factor during storms, *J. Waterw.
Coastal Port Ocean Eng.*, 129, 174–177, doi:10.1061/(ASCE)0733-
950X(2003)129:4(174).
Lewis, E. R., and S. E. Schwartz (Eds.) (2004), *Sea Salt Aerosol Produc-
tion: Mechanisms, Methods and Measurements and Models—A Critical
Review, Geophys. Monogr. Ser.*, vol. 152, AGU, Washington, D. C.
Monahan, E. C. (1969), Fresh water whitecaps, *J. Atmos. Sci.*, 26,
1026–1029.
Monahan, E. C., and M. Lu (1990), Acoustically relevant bubble assem-
blages and their dependence on meteorological parameters, *IEEE J.
Oceanic Eng.*, 15, 340–349.
Monahan, E. C., and I. O'Muircheartaigh (1980), Optimal power-law
description of oceanic whitecap coverage dependence on wind speed,
J. Phys. Oceanogr., 10, 2094–2099.
Monahan, E. C., and D. K. Woolf (1989), Comments on "Variations of
whitecap coverage with wind stress and water temperature," *J. Phys.
Oceanogr.*, 19, 706–709.
Monahan, E. C., C. W. Fairall, K. L. Davidson, and P. J. Boyle (1983),
Observed inter-relations between 10m winds, ocean whitecaps and mar-
ine aerosols, *Q.J.R. Meteorol. Soc.*, 109, 379–392.
Monahan, E. C., D. E. Spiel, and K. L. Davidson (1986), A model of marine
aerosol generation via whitecaps and wave disruption, in *Oceanic White-
caps and Their Role in Air-Sea Exchange Processes*, edited by E. C.
Monahan and G. MacNiochaill, pp. 167–174, Springer, New York.
Nordberg, W., J. Conaway, D. B. Ross, and T. Wilheit (1971), Measure-
ments of microwave emission from a foam covered, wind-driven sea,
J. Atmos. Sci., 28, 429–435.
O'Dowd, C. D., and G. de Leeuw (2007), Marine aerosol production: A
review of current knowledge, *Philos. Trans. R. Soc., Ser. A*, 365,
1753–1774.
Ross, D. B., and V. Cardone (1974), Observations of oceanic whitecaps and
their relation to remote measurements of surface wind speed, *J. Geophys.
Res.*, 79, 444–452.
Stramska, M., and T. Petelski (2003), Observations of oceanic whitecaps in
the north polar waters of the Atlantic, *J. Geophys. Res.*, 108(C3), 3086,
doi:10.1029/2002JC001321.
Sugihara, Y., H. Tsumori, T. Ohga, H. Yoshioka, and S. Serizawa (2007),
Variation of whitecap coverage with wave-field conditions, *J. Mar. Syst.*,
66, 47–60.
Woolf, D. K. (2005), Parameterization of gas transfer velocities and sea-
state-dependent wave breaking, *Tellus, Ser. B*, 57, 87–94.

————————————
A. Callaghan, Department of Earth and Ocean Sciences, National
University of Ireland, University Road, Galway, Ireland. (callaghan.
adrian@gmail.com)
L. Cohen, TNO Defense and Security, P.O. Box 96864, NL-2509 JG
Hague, Netherlands.
G. de Leeuw, Department of Physics, University of Helsinki, P.O.Box 64,
FIN-00014 Helsinki, Finland.
C. D. O'Dowd, School of Physics and Centre for Climate and Air
Pollution Studies, Environmental Change Institute, National University of
Ireland, University Road, Galway, Ireland.